Organic & Biomolecular Chemistry

Dynamic Article Links

Cite this: *Org. Biomol. Chem.*, 2011, **9**, 6917

www.rsc.org/obc

COMMUNICATION

Multifunctional small molecule for controlled assembly of oligomeric nanoparticles and crosslinked polymers†

Yun Deng, Shuang Liu, Kun Mei, An-ming Tang, Chun-yan Cao and Gao-lin Liang*

Received 9th July 2011, Accepted 15th August 2011
DOI: 10.1039/c1ob06132a

One multifunctional small molecule can undergo a natural condensation reaction under the control of reducing agent to generate amphiphilic oligomers which quickly self-assemble supramolecular nanoparticles or form crosslinked, reversibly degradable polymers.

In nature, self-assembling small molecules through non-covalent or covalent bonds to build up supramolecular structures (normally nanometre-sized) is a prevalent and important process.[1] Imitating nature, chemists assemble building blocks (usually small molecules, sometimes polymers) in physiological solution to make biocompatible supramolecular materials for controlled drug release and delivery,[2] biosensing,[3] tissue engineering,[4] and wound healing.[5] In spite of the frequent observation of nanostructures which are formed *via* the assembly of the oligomers from biological macromolecules in nature by biologists,[6] using oligomers to assemble nanostructures *in vitro* has remained less exploited by chemists. Recently, Rao and co-workers have developed a biocompatible condensation reaction between the 1,2-aminothiol group of cysteine and the cyano group of 2-cyanobenzothiazole (CBT) in physiological solution which could be controlled by pH, reduction, or protease.[7] One merit of this controllable condensation reaction is that it offers relatively more hydrophobic, macrocyclic, oligomeric, biocompatible products for self-assembling nanostructures, which promises its potential for applications on the assembly of nanostructures with oligomers. Another valuable feature of this condensation system is that it has a high second-order rate constant (9.19 M^{-1} S^{-1} for the condensation reaction between amino-CBT and free cysteine), which is significantly larger than that of a biocompatible click reaction (7.6×10^{-2} M^{-1} S^{-1}).[8] Thus, we postulate that inserting functional groups (motifs) between the CBT and cysteine motifs probably would not affect the condensation. The middle functional motif could be a fluorescent probe for cellular or animal optical imaging, DOTA-Gd for magnetic resonance imaging (MRI), radioactive isotope for nuclear imaging, anti-cancer drug for killing cancer cells, *et al.*

Inspired by this, as shown in Scheme 1, we designed Cys(SEt)-Lys(Cys(SEt))-CBT (**1**) for reduction-controlled condensation to produce amphiphilic oligomers in water at pH 7.4. Due to the π–π stacking of their aromatically hydrophobic cores and the hydrogen bonds between their cysteinic arms and surrounding water, the oligomers quickly self-assemble into nanoparticles. Interestingly, purified oligomers are easily oxidized to form crosslinked polymers because the cysteinic arms of the oligomers "grab" at each other to form disulfide linkages after oxidation. As-formed crosslinked polymers are hardly dissolved in laboratory solvents. Nevertheless, when sonicated with TCEP in water, the crosslinked polymers could be partially degraded into their starting oligomers. Thus, by carefully designing a multifunctional small molecule (*i.e.*, **1**) and applying it to the versatile condensation reaction, we successfully manipulated **1** from monomers to oligomers, polymers, and nanoparticles. The thiol groups of the two cysteinic motifs of **1** are disulfided not only for stabilizing the compound in physiological solution but also for latent reductions by reducing reagents such as TCEP mentioned in this paper, dithiothreitol (DTT) in biological working buffer, glutathione (GSH) in cells.

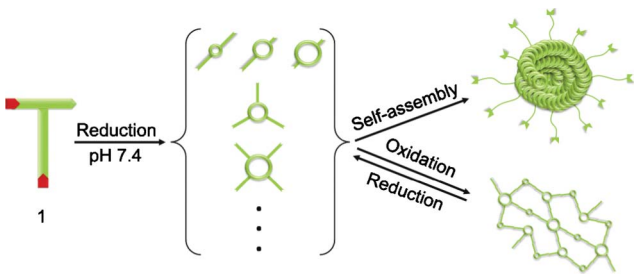

Scheme 1 Reduction controlled condensation for self-assembly of oligomeric nanoparticles and crosslinked polymers.

We began the study with reduction controlled condensation and self-assembly of nanoparticles. Together with **1**, Cys(SEt)-Lys(Biotin)-CBT (**2**) was also studied in parallel to study the influence of the hydrophilic properties of the precursors on the formation of their oligomeric products and the morphologies of the nanostructures self-assembled afterwards (Fig. 1). The structural difference between **1** and **2** is the motif modified on the side chain of the middle lysine, that is, cysteine for **1** and biotin for **2**. Thus, **1** is more hydrophilic than **2**. At the concentration

CAS Key Laboratory of Soft Matter Chemistry, National Synchrotron Radiation Laboratory, Department of Chemistry, University of Science and Technology of China, 96 Jinzhai Road, Hefei, Anhui 230026, China. E-mail: gliang@ustc.edu.cn; Fax: +86-551-3600730; Tel: +86-551-3607935

† Electronic supplementary information (ESI) available: Experimental details, synthesis of **1,2**, UV-Vis, HPLC conditions, MALDI mass spectra, SEM, TEM, supplementary figures (Fig. S1–S10). See DOI: 10.1039/c1ob06132a

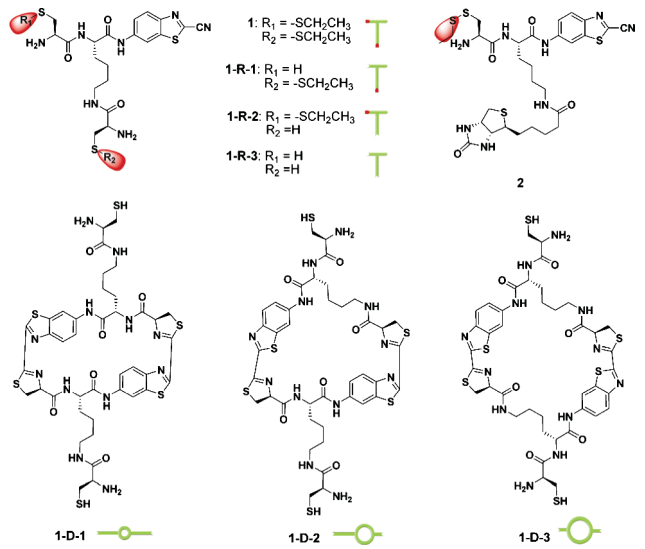

Fig. 1 Chemical structures of **1**, its reduced products (**1-R-1**, **1-R-2**, and **1-R-3**), three conformations of its dimmers after condensation (**1-D-1**, **1-D-2**, and **1-D-3**), and **2**.

of 1 mM, **1** and **2** were dissolved in water. 5 min after adding 4 equiv. of TCEP for **1** and adjusting the pH value to 7.4 with sodium carbonate, we observed that the clear solution of **1** became a turbid dispersion (Fig. 2a) and its UV-Vis spectra at 500–700 nm showed an obvious increase of absorption suggesting the aggregation of particles (Fig. S1, ESI†). Dynamic light scattering (DLS) measurement indicated that the nanoparticles have a mean dynamic diameter of 52.5 nm (Fig. 2b).

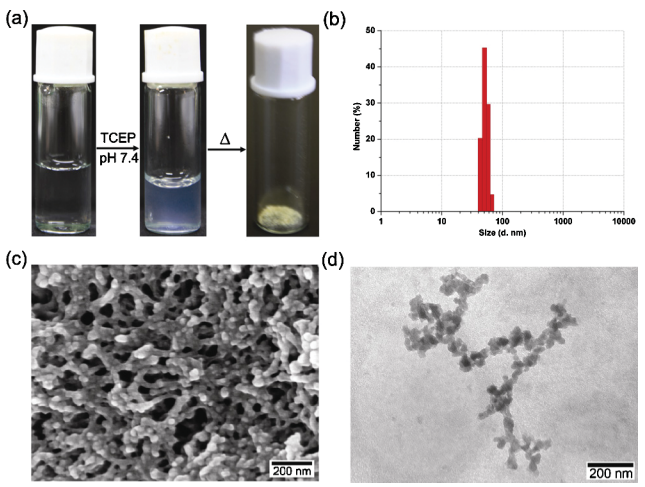

Fig. 2 (a) Photographs of the solution of **1** at 1 mM dissolved in water (left), the dispersion of nanoparticles of its condensation products after the addition of 4 equiv. of TCEP and adjusting the pH to 7.4 for 5 min (middle), and crosslinked polymer obtained after the oligomers had being purified and heated at 50 °C (right). (b) Dynamic light scattering (DLS) analysis of particle-size distribution of the self-assembled condensation products of **1**. (c, d) SEM and TEM images of the nanoparticles in the dispersion of a.

Directly taking the above dispersion for scanning electron microscope (SEM) and transmission electron microscope (TEM) observation, we uncovered the 3-dimensional and 2-dimensional depositions of the nanoparticles. The nanoparticles of **1** have an average diameter of 27–43 nm and tend to connect with each other to form nanofibers which entangle to buildup 3-dimensional porous structures (Fig. 2c&d).

Unlike the behavior of the nanoparticles of **1** above, condensation of **2** results in separated, bigger nanoparticles which have an average diameter of 100–156 nm (Fig. S2, ESI†). This might be due to the fact that the condensation products of **2** are more hydrophobic than those of **1** and tend to aggregate faster to form separated bigger nanoparticles. Matrix-assisted laser desorption/ionization (MALDI) mass spectroscopic analysis of the reaction mixture of **2** revealed that only the dimer of **2** was detected (Fig. S3, ESI†). In contrast, a lot of ionic peaks of the oligomers of **1** ranging from dimer, trimer, tetramer, to even higher order oligomers appeared on the MALDI mass spectra of **1**, indicating that more hydrophilic precursors are prone to producing higher order oligomers and self-assembling nanofibers under this condensation. Interestingly, while the condensation of **2** only offers big nanoparticles, condensation products of **1** (*i.e.*, oligomers of **1**) can be further used for the preparation of crosslinked polymers because their cysteinic arms are ready for disulfide linkage. After the condensation of **1**, we dissolved the reaction mixture in methanol and ran it through a HPLC column. All the oligomeric products were collected and the eluent was evaporated at 50 °C resulting in a yellowish, amorphous, polymeric powder which is insoluble in laboratory solvents (Fig. 2a). Each purified oligomer (*e.g.*, **1-D-3**) can also individually produce polymers with similar properties under the same condition. Interestingly, when TCEP was added into the water suspension of the polymers of **1-D-3** and sonicated, we clearly observed that the **1-D-3** peak reappeared on the HPLC trace, suggesting the tunability of the "oligomer–polymer" process (Fig. 3d&e).

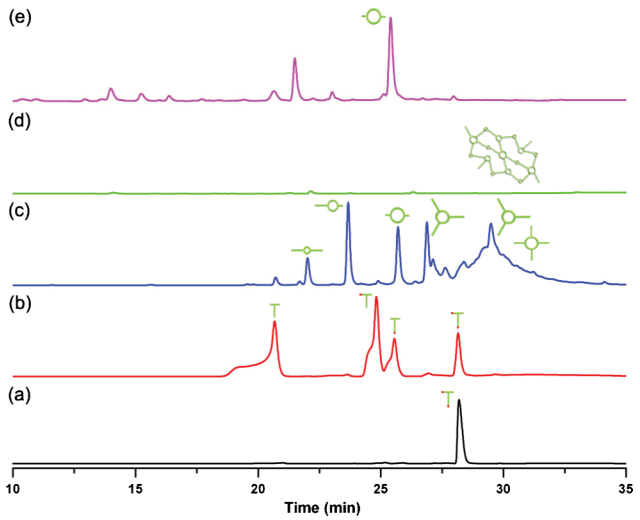

Fig. 3 HPLC traces of (a) **1**, (b) 1 mM of **1** with 4 equiv. of TCEP in water at pH 2 for 30 min indicating the formation of reduced products of **1-R-1**, **1-R-2**, and **1-R-3**, (c) Self-assembled nanoparticles of the condensation products of **1** dissolved in methanol showing the oligomeric products are **1-D-1**, **1-D-2**, **1-D-3**, and higher order oligomers, (d) Crosslinked polymers of **1-D-3** (25.7 min in c) extracted with methanol, and (e) Polymers in d sonicated with 4 mM TCEP in water for 30 min indicating the defragmentation of the polymers and the recovery of **1-D-3**. The Y-axis of e was adjusted at the same scale as that of d.

Analysis of HPLC traces together with MALDI mass spectra successfully revealed the whole processes of reduction of **1** to generate three reduced products, self-assembly of the oligomeric mixtures to form nanoparticles, formation of insoluble crosslinked polymers, and the degradation of the polymers with TCEP (Fig. 3). Firstly, we divided the condensation of **1** at pH 7.4 into two steps. When the pH value is below 4, the condensation between free cysteine and CBT won't happen but TCEP still has weak ability of reduction.[9] As shown in Fig. 3b, reduction of 1 mM of **1** with 4 equiv. of TCEP in water at pH 2 for 30 min indeed produces three reduced products: **1-R-1** (15.3%), **1-R-2** (32.0%), and **1-R-3** (41.4%, confirmed by MALDI mass spectrum in Fig. S4, ESI†). After that, the pH value was raised to 7.4 and the condensation happened resulting in a dispersion of nanoparticles. With the addition of methanol, the dispersion changed to a clear solution and was injected into a HPLC system for analysis. Together with the analysis of their MALDI mass spectra, we identified the peaks in Fig. 3c at the retention times of 22.0, 23.7, and 25.7 min as **1-D-1** (3.4%), **1-D-2** (10.5%), and **1-D-3** (8.6%), the peak at 26.9 min as the trimer of **1** (8.3%), and the broad peak around 29.5 min as higher order oligomeric mixtures of **1** (*e.g.*, tetramer, pentamer, *et al.* 64.6%) respectively (Fig. S5, ESI†). Collecting the peak of **1-D-3** at 25.7 min in Fig. 3c and evaporating the solvent at 50 °C, we obtained the same yellowish polymers as Fig. 2a which are also insoluble in laboratory solvents (Fig. 3d). However, resuspending the polymers of **1-D-3** in 4 mM TCEP solution and sonicating the mixture, we observed the partial degradation of the polymer and the reappearance of the peak of **1-D-3** on the HPLC trace (Fig. 3e). This indicates that the degradation of the insoluble polymers crosslinked *via* disulfide linkage is still feasible under the action of reducing agents (*e.g.*, TCEP, glutathione, DTT) or reductase.

Besides other techniques such as 2-dimensional nuclear magnetic resonance (2D-NMR) employed for the characterizations of the formation of macrocyclized rings,[7a] herein we used infrared (IR) measurement to monitor the evolution of **1**, from monomer to its oligomers and crosslinked polymers. As shown in Fig. 4a, the IR spectrum of **1** has a typical nitrile peak at 2232.29 cm^{-1} and weak broad peak at 426.27 cm^{-1} identified as its disulfide bond. After the purification of the nanoparticles from the dispersion in Fig. 2a by centrifugation, the IR spectrum of the mixture of nanoparticles shows disappearance of the peaks of nitrile and disulfide bonds, and obvious appearance of a peak at 1660.11 cm^{-1} corresponding to the stretching frequency of C═N (Fig. 4b). This proved the occurrence of the condensation between the cyano group of **1** with its 1,2-aminothiol group to form a thiazole ring after TCEP reduction. Compared with that of the oligomeric mixtures, the IR spectrum of the yellowish polymers shows an enhanced peak at 1037.28 cm^{-1} which could be characterized as C–C–C bending due to the connection of the cysteinic arms of the oligomers and the reappearance of the disulfide bond at 432.06 cm^{-1} ascribed to the formation of disulfide linkage between the oligomers.

In summary, by carefully designing a multifunctional small molecule (*i.e.*, **1**) and applying it to a versatile condensation reaction developed, we successfully manipulated the molecule of **1** among monomers, oligomers, polymers, and nanostructures. Compared with other systems for producing polymers from oligomers,[10] our strategy offers a controllable and reversible process of polymerization. Moreover, with the free cysteinic arms extending on their surfaces, the nanoparticles of **1** might find future applications such as protein labeling, cellular imaging, and so on. Related research works are underway.

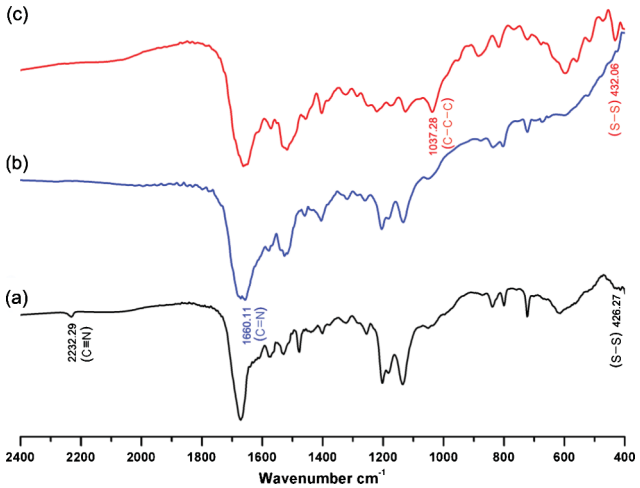

Fig. 4 IR spectra of (a) **1**, (b) Purified nanoparticles of **1** in the dispersion of Fig. 2a, and (c) Crosslinked polymers in Fig. 2a.

This work was partially supported by the Start-up funding of USTC (ZC9850290065 and W21103030901), National Science Foundation of China (21045002), Anhui Provincial Natural Science Foundation (11040606M178), Chinese Universities Scientific Fund, and Program for New Century Excellent Talents in University.

Notes and references

1 (*a*) G. M. Whitesides, J. P. Mathias and C. T. Seto, *Science*, 1991, **254**, 1312; (*b*) G. A. Silva, C. Czeisler, K. L. Niece, E. Beniash, D. A. Harrington, J. A. Kessler and S. I. Stupp, *Science*, 2004, **303**, 1352.
2 (*a*) S. Koutsopoulos, L. D. Unsworth, Y. Nagaia and S. G. Zhang, *Proc. Natl. Acad. Sci. U. S. A.*, 2009, **106**, 4623; (*b*) G. L. Liang, Z. M. Yang, R. J. Zhang, L. H. Li, Y. J. Fan, Y. Kuang, Y. Gao, T. Wang, W. W. Lu and B. Xu, *Langmuir*, 2009, **25**, 8419.
3 (*a*) M. G. Shapiro, J. O. Szablowski, R. Langer and A. Jasanoff, *J. Am. Chem. Soc.*, 2009, **131**, 2484; (*b*) I. Hamachi, T. Nagase and S. Shinkai, *J. Am. Chem. Soc.*, 2000, **122**, 12065; (*c*) G. L. Liang, K. M. Xu, L. H. Li, L. Wang, Y. Kuang, Z. M. Yang and B. Xu, *Chem. Commun.*, 2007, 4096.
4 V. Jayawarna, M. Ali, T. A. Jowitt, A. E. Miller, A. Saiani, J. E. Gough and R. V. Ulijn, *Adv. Mater.*, 2006, **18**, 611.
5 Z. M. Yang, G. L. Liang, M. L. Ma, A. S. Abbah, W. W. Lu and B. Xu, *Chem. Commun.*, 2007, 843.
6 M. M. Murr and D. E. Morse, *Proc. Natl. Acad. Sci. U. S. A.*, 2005, **102**, 11657.
7 (*a*) G. L. Liang, H. J. Ren and J. H. Rao, *Nat. Chem.*, 2010, **2**, 54; (*b*) H. J. Ren, F. Xiao, K. Zhan, Y. P. Kim, H. X. Xie, Z. Y. Xia and J. Rao, *Angew. Chem., Int. Ed.*, 2009, **48**, 9658; (*c*) D. J. Ye, G. L. Liang, M. L. Ma and J. H. Rao, *Angew. Chem., Int. Ed.*, 2011, **50**, 2275; (*d*) G. L. Liang, J. Ronald, Y. X. Chen, D. J. Ye, P. Pandit, M. L. Ma, B. Rutt and J. H. Rao, *Angew. Chem., Int. Ed.*, 2011, **51**, 6283.
8 J. M. Baskin, J. A. Prescher, S. T. Laughlin, N. J. Agard, P. V. Chang, I. A. Miller, A. Lo, J. A. Codelli and C. R. Bertozzi, *Proc. Natl. Acad. Sci. U. S. A.*, 2007, **104**, 16793.
9 D. J. Cline, S. E. Redding, S. G. Brohawn, J. N. Psathas, J. P. Schneider and C. Thorpe, *Biochemistry*, 2004, **43**, 15195.
10 M. S. El-Shall, *Acc. Chem. Res.*, 2008, **41**, 783.